

Published in final edited form as:

Int J Pharm. 2013 February 28; 444(0): 185–192. doi:10.1016/j.ijpharm.2013.01.001.

Application of Knockout Mouse Models to Investigate the Influence of Fc γ R on the Pharmacokinetics and Anti-Platelet Effects of MWReg30, a Monoclonal Anti-GPIIb Antibody

Lubna Abuqayyas, Xiaoyan Zhang, and Joseph P. Balthasar

Department of Pharmaceutical Sciences, School of Pharmacy and Pharmaceutical Sciences, University at Buffalo, the State University of New York, Buffalo, New York 14260, USA

Abstract

This work evaluates the influence of Fc γ R on the pharmacokinetics and pharmacodynamics of a rat anti-integrin- α IIb IgG1 monoclonal antibody, MWReg30, in mice. The pharmacokinetics and pharmacodynamics of MWReg30 were investigated in C57BL/6 control mice, Fc γ RI/RIII knockout mice, and Fc γ RIIb knockout mice, following intravenous doses of 0.04 – 0.4 mg/kg. MWReg30 treatment resulted in a dose-dependent induction of thrombocytopenia in all strains, but sensitivity to MWReg30 was increased in Fc γ RIIb knockout mice and decreased in Fc γ RI/RIII knockout mice, relative to results found in control mice. Expressed as a percentage of pre-treatment platelet counts, nadir platelet counts were 28.6 \pm 5.0, 88.7 \pm 16.6 and 25.3 \pm 6.1% at 0.05 mg/kg, 28.4 \pm 13.7, 56.7 \pm 5.1, and 20.6 \pm 9.5% at 0.2 mg/kg, and 24.9 \pm 7.2, 38.7 \pm 7.5, and 7.4 \pm 2.2% at 0.4 mg/kg in control, Fc γ RI/RIII(-/-) and Fc γ RIIb(-/-) mice. However, knocking out Fc γ R did not affect MWReg30 pharmacokinetics. Plasma areas under the concentration vs. time curves (AUC_{0-10days}) \pm SD for MWReg30 were: 5.24 \pm 0.68, 5.51 \pm 0.24, and 5.39 \pm 1.05 nM \times d at 0.04 mg/kg, and 12.7 \pm 0.5, 13.6 \pm 1.1, and 14.5 \pm 2.0 nM \times d at 0.1 mg/kg in control, Fc γ RI/RIII(-/-) and Fc γ RIIb(-/-) mice. The findings further emphasize the role of activating vs. inhibitory Fc γ R in processing immune complexes (i.e., MWReg30-platelets), while also providing an example where monoclonal antibody pharmacokinetics are not substantially influenced by Fc γ R expression.

Keywords

Anti-platelet antibody; IgG; Fc γ -receptors; pharmacokinetics; pharmacodynamics; tissue disposition

1. Introduction

Several classes of Fc γ R have been identified in man and in mouse, including receptors that activate effector functions (i.e., Fc γ RI, Fc γ RIIA, and Fc γ RIIIA) and receptors that inhibit effector functions (Fc γ RIIb) (Nimmerjahn et al., 2005; Nimmerjahn and Ravetch, 2008; Siberil et al., 2007; Tarasenko et al., 2007). Immunoglobulin G (IgG) binds with high

© 2013 Elsevier B.V. All rights reserved

Corresponding Author: Joseph P. Balthasar, 452 Kapoor Hall, Department of Pharmaceutical Sciences, School of Pharmacy and Pharmaceutical Sciences, University at Buffalo, the State University of New York, Buffalo, New York 14260, USA. Phone: +1716 645 4807; Fax: +1716 645 369, jb@buffalo.edu.

Publisher's Disclaimer: This is a PDF file of an unedited manuscript that has been accepted for publication. As a service to our customers we are providing this early version of the manuscript. The manuscript will undergo copyediting, typesetting, and review of the resulting proof before it is published in its final citable form. Please note that during the production process errors may be discovered which could affect the content, and all legal disclaimers that apply to the journal pertain.

affinity (10^{-8} – 10^{-9} M) to Fc γ RI, and with lower affinity to Fc γ RIIA, Fc γ RIIb, and Fc γ RIII (10^{-7} – 10^{-8} M). Activating and inhibitory Fc γ R are expressed on cells of hematopoietic origin (i.e., beta cells, basophils, T-lymphocytes, monocytes, and mast cells), and in antigen-presenting cells that include dendritic cells and macrophages (Amigorena and Bonnerot, 1999a, b; Cassel et al., 1993; Nimmerjahn and Ravetch, 2006; Ravetch and Bolland, 2001). Large populations of cells expressing Fc γ R are found in the bone marrow, thymus, lung, liver, and spleen (Bhatia et al., 1998; Bordessoule et al., 1993; Ivan and Colovai, 2006; Tuijnman et al., 1993; Van de Winkel and Capel, 1993).

The binding of the Fc domain of IgG antibodies to activating Fc γ R leads to several immune responses, such as antibody-dependent cell cytotoxicity, the release of inflammatory molecules (such as cytokines), enhancement of antigen presentation, and phagocytosis of immune complexes (Nimmerjahn and Ravetch, 2006, 2008; Siberil et al., 2007; Tarasenko et al., 2007). IgG immune complexes or IgG opsonized particles are rapidly engulfed upon binding to Fc γ R on macrophages and dendritic cells, leading to the elimination of associated particles or antigens.

Immune thrombocytopenic purpura (ITP) is an autoimmune condition where patients develop autoantibodies with affinity for platelet membrane glycoproteins (e.g., GPIIb/IIIa and GPIb/IX) (Van Leeuwen et al., 1982). Antibody-opsonized platelets are eliminated by phagocytic cells of the reticuloendothelial system, in tissues such as the spleen and liver (Cines and Blanchette, 2002). Due to the well-known role of Fc γ R in the elimination of immune complexes and opsonized particles, and due to the moderate-to-high affinity of monomeric IgG for Fc γ R, it has been assumed that Fc γ R play an important role in the elimination and tissue distribution of all IgG antibodies (McDonagh et al., 2008; Mould and Green, 2010; Nishio et al., 2009; Tabrizi et al., 2010; Tabrizi et al., 2006; Zuckier et al., 1994). Although there has been wide acceptance of the hypothesis that Fc γ R are key determinants of IgG pharmacokinetics (PK), this supposition has not been thoroughly examined within the published literature.

Recently, we evaluated the effect of Fc γ R on the elimination and tissue distribution of 8C2, a model monoclonal IgG1 antibody with high affinity for a soluble ligand (topotecan). Our results demonstrated virtually identical 8C2 plasma and tissue disposition in wild-type mice and in Fc γ R knock-out mice (Abuqayyas and Balthasar, 2012, in press). To evaluate the role of Fc γ receptors as determinants of the disposition and pharmacodynamics (PD) of a model monoclonal antibody with specific affinity for cell surface proteins (i.e., forming opsonized cells), we have now assessed the PK and PD of MWReg30 in control (wild-type) mice and Fc γ R-knockout mice. MWReg30, which is a rat IgG1 mAb with high affinity for mouse integrin α IIB (GPIIb), has been shown to induce thrombocytopenia in mice, and has been used to develop mouse models of ITP (Deng and Balthasar, 2007).

2. Material and methods

2.1. Materials

MWReg30 was purchased from BD Pharmingen™ (San Diego, CA). Sodium iodide (Na-¹²⁵I) was obtained from Perkin Elmer Inc. (Waltham, MA). Chloramine-T, sodium metabisulfite, calcium sulphate (CaSO₄), and carboxymethyl cellulose (CMC) were from Sigma Life Science (St Louis, MO). Potassium iodide (KI) and sodium iodide (Na-¹²⁷I) were from Fischer Scientific (Pittsburgh, PA). MWReg30 was labeled with ¹²⁵I via the Chloramine-T method, as described previously (Garg and Balthasar, 2007). The purity of the iodinated IgG was assessed using instant thin layer chromatography (PE SiL-G, Whatman Ltd, Kent, England), as described previously (Garg and Balthasar, 2007). For all experiments, the purity of the iodinated preparation was higher than 99%.

2.2. Animals

B6.129P2-*FcγRIg^{tm1Rav}* N12 mice, deficient in the gamma chain subunit of the FcγRI and FcγRIII receptors (FcγRI/RIII(-/-)), B6.129S4-*FcγRIIb^{tm1TiK}* N12, a mouse knockout for the inhibitory receptor, FcγRIIb (FcγRIIb(-/-)), and control C57BL/6 wild type (WT) strains were purchased from Taconic Laboratories (Hudson, NY). Swiss Webster mice were obtained from Harlan Laboratories (Indianapolis, IN). Mice were housed under a standard artificial light/dark cycle, with free access to food and water, and under controlled temperature and humidity. Mice were allowed to acclimate to the animal unit for at least a week prior to investigation. Mice were also kept on autoclaved KI-water (0.2 g/L) to block the thyroidal uptake of free iodine, beginning 2 days prior to injection of ¹²⁵I-MWReg30. All animal protocols were conducted with approval from the Institutional Animal Care and Use Committee of the State University of New York at Buffalo.

2.3. Methods

2.3.1. Assessment of MWReg30-mediated thrombocytopenia in C57BL/6, FcγRI/III(-/-), and FcγRIIb(-/-) mice—MWReg30 was administered intravenously to groups of C57BL/6, FcγRI/RIII(-/-), and FcγRIIb(-/-) mice, at doses of 0.05, 0.2 and 0.4 mg/kg, via penile vein injection (n=5–7 mice / dose / strain). Blood samples were collected from the retro-orbital plexus prior to dosing for determination of baseline platelet measurements. Additional samples were obtained at several time points up to 3 days post dosing. Blood samples were collected using ethylenediaminetetraacetic acid coated capillary pipette tubes. Platelet counts were determined using a Cell-Dyn 1700 multi-parameter hematology analyzer (Abbott Laboratories, Abbott Park, IL), normalized by the baseline platelet counts, and reported as a percentage of pretreatment values.

2.3.2. Effect of iodination on MWReg30-mediated thrombocytopenia—MWReg30 was iodinated with ¹²⁷I (non-radioactive iodine) using the Chloramine-T modified method (Garg and Balthasar, 2007). MWReg30 or ¹²⁷I- MWReg30, at a dose of 0.2 mg/kg, was injected intravenously via the penile vein into two groups of Swiss Webster mice (6–7 weeks old, n=3/group). Blood samples were collected before treatment and at 1, 3, 6, 9, 24 and 72 h after treatment. Ten μL blood samples were collected from the retro-orbital plexus and/or the submandibular vein using ethylenediaminetetraacetic acid pre-coated capillary pipette tubes. Platelet counts were determined using a Cell-Dyn Emerald (Abbott Laboratories, Abbott Park, IL).

2.3.3. Assessment of MWReg30 plasma pharmacokinetics in C57BL/6, FcγRI/III(-/-), and FcγRIIb(-/-) mice—The pharmacokinetics of MWReg30 mAb were evaluated at 0.04, 0.1, and 0.4 mg/kg in C57BL/6, FcγRI/RIII(-/-), and FcγRIIb(-/-) mice (20–22 g). MWReg30 was administered as a mixture of the indicated MWReg30 dose plus a tracer amount (<10% of total dose) of ¹²⁵I-MWReg30 (~10 μCi/mouse). The mAb was administered intravenously via the penile vein (n= 3–5 mice per dose per strain). Blood samples, ~20–40 μL, were collected from the retro-orbital plexus or from the submandibular vein at 1 h, 3 h, 8 h, and at 1, 2, 4, 7 and 10 days. Plasma was separated, and counted for radioactivity using a gamma counter (LKB Wallac 1272, Wallac, Turku, Finland). Radioactive counts were corrected for decay and background, and MWReg30 plasma concentrations were determined. Of note, in prior work with intravenous administration of ¹²⁵I-labeled monoclonal antibodies to mice, we have found that more than 95% of plasma and tissue radioactivity is trichloroacetic acid (TCA) precipitable, up to 10 days post injection, supporting the use of ¹²⁵I-labeling for evaluating mAb pharmacokinetics in mice (Garg and Balthasar, 2007). In the current study, the efficiency of TCA precipitation was evaluated in samples collected on day 14.

2.3.4. Assessment of MWReg30 tissue distribution—Fourteen days following injection of 0.1 mg/kg ^{125}I -MWReg30, 3 mice from each strain were sacrificed. Blood, spleen, kidney, liver, heart, lung, thymus, GI, muscle, bone, fat and skin samples were harvested, and radioactivity was counted. MWReg30 concentrations in excised tissues were determined following correction for background and decay.

2.3.5. Non-compartmental data analysis—Non-compartmental pharmacokinetic analysis (NCA) (WinNonlin 6.1, Phoenix, Pharsight Corporation, Palo Alto, CA) was used to analyze MWReg30 plasma concentration vs. time data. MWReg30 plasma clearance (CL), mean areas under the concentration vs. time curves ($\text{AUC}_{0-10\text{days}}$), and volume of distribution at steady-state (V_{ss}) were obtained. For each dose, 3–5 mice per strain were used. The pharmacokinetic parameters were reported as mean \pm standard deviation (SD). MWReg30 tissue to blood concentration ratios were determined, and the mean of the ratios and SD were reported.

2.3.6. Analysis of effect of dose on MWReg30-mediated thrombocytopenia—

To characterize the induction of thrombocytopenia across the strains, the relationship between the % change in platelet counts at the nadir vs. MWReg30 dose was fitted to the Hill equation (equation 1), with use of mixed-effect modeling with NONMEM (ICON Development Solutions Ellicott City, Maryland). Due to the sparseness of the data, the first-order estimation method was employed. The magnitude of unexplained inter-animal variability in model parameters, as well as the magnitude of unexplained residual variability, were estimated. A log-normal distribution was assumed for inter-animal variability of model parameters, and an additive error model was used to describe unexplained residual variability.

$$E = E_0 + \frac{E_{\text{max}} \times \text{Dose}}{ED_{50i} + \text{Dose}} \quad (1)$$

In this equation, E represents the % change in the platelet counts at the nadir, E_0 is initial change in % platelet counts when no drug was administered, E_{max} is the maximal achieved effect, and ED_{50} is the dose associated with 50% change in the platelet counts. Data from all strains were modeled simultaneously. E_0 was fixed to zero, assuming no changes when no drug was administered. The effect of strain as a predictor of model parameters was explored. A likelihood ratio test was used to assess statistical significance of each covariate effect within NONMEM® using stepwise forward selection ($\alpha = 0.05$), followed by stepwise backward elimination ($\alpha = 0.001$) procedures.

2.3.7. Analysis of MWReg30 plasma pharmacokinetics—One-compartment and two-compartment mammillary models were used to characterize MWReg30 plasma pharmacokinetics in control, $\text{Fc}\gamma\text{RI/III}(-/-)$, and $\text{Fc}\gamma\text{RIIb}(-/-)$ mice. The model with optimal fitting criteria was selected for more data analysis. The structure of the two compartment model is presented in Figure 1. The model consists of a central compartment and a peripheral distribution compartment. MWReg30 elimination is assumed to occur only from the central compartment. Linear distribution to and from the peripheral distribution compartment were assumed. The data from all strains at all dose levels were fit simultaneously using equations 2 and 3.

$$V_c \times \frac{dc_c}{dt} = CL_d \times C_t - (CL_d + CL_c) \times C_c \quad (2)$$

$$V_t \times \frac{dC_t}{dt} = CL_d \times C_c - CL_d \times C_t \quad (3)$$

MWReg30 plasma and tissue concentrations are symbolized as C_c and C_t . CL_c represents the elimination clearance, and CL_d represents the distribution clearance between the central and peripheral compartments. V_c and V_t are the volumes of distribution for the central and tissue compartments. Model fitting was performed using a population nonlinear mixed effect modeling approach in NONMEM 7. The first order conditional estimation method, ADVAN3, and TRANS4 were used. Structural model parameters, the magnitude of inter-animal variability in these parameters, and the magnitude of residual variability were estimated. Incorporation of inter-animal variability was evaluated for all model parameters. Inter-animal variability was described using an exponential variance model:

$$P_j = P_{pop} \times \exp(\eta_j) \quad (4)$$

P_j and P_{pop} represent parameters for the j^{th} animal and the typical animal value, η_j is the inter-animal variability in the j^{th} animal, with a normal distribution around 0 and variance of ω^2 . The exponential model assumes a log-normal distribution of the parameters. Residual variability was described using a constant coefficient of variation (proportional) error model:

$$C_{ij} = \widehat{C}_{ij} \times (1 + \varepsilon_{ij}) \quad (5)$$

C_{ij} represents the measured plasma concentration at the i^{th} time-point in the j^{th} animal; \widehat{C}_{ij} is the model predicted MWReg30 plasma concentration at the i^{th} time-point in the j^{th} animal, and E_{ij} is a random variable representing discrepancy between the i^{th} measurement in the j^{th} animal and the predicted value. E_{ij} is assumed to be normally distributed with a mean of 0 and variance of σ_{prop}^2 . The precision of the parameter estimates were expressed as the standard error of the mean (SEM). Covariate analyses were performed on all model parameters using forward selection and backward elimination methods. An additive shift was used to describe the relationship between strain and the relevant pharmacokinetics parameter. A 3.84 drop in the mean value of objective function (MVOF) was required to compare two nested models. This value corresponds to a p-value of 0.05, for the addition of a single parameter, based on a χ^2 -distribution. In the forward selection, the covariate that was associated with the most significant change in the MVOF was included to form the new base covariate model. This process was repeated until there were no further covariates that produced significant changes in the MVOF. Visual predictive checks (VPC) were used to evaluate whether the fixed and random effects of the final model adequately described the observed pharmacokinetic data. VPCs are based on simulations of model predictions, conditional on fixed and random effect final estimates, including significant covariates, if any. Identical dosing and sampling schemes for all dose groups were used for simulations. 500 replicates of the analysis dataset design and dosing schemes were simulated. The simulated population median and the 5th and 95th percentiles (90% prediction interval) were calculated. The observed concentrations and the population prediction interval were overlaid to allow visual comparisons of the central tendencies for observed and predicted data. Simulation-based plots were stratified by dose.

2.3.8. Statistical analysis—The NCA-calculated pharmacokinetic parameters and concentration ratios in C57BL/6, Fc γ RI/RIII(−/−), and Fc γ RIIb(−/−) mice were statistically compared using one-way Analysis of Variance (ANOVA). A significance level of $\alpha = 0.05$ was assumed (Graph Pad Prism 5, Graph Pad, San Diego, CA). Bonferroni's correction was

used to allow multiple comparisons of different groups (C57BL/6 vs. γ R111(-/-) and C57BL/6 vs. γ R11b(-/-)). Student's t-test was also used with $\alpha = 0.05$.

3. Results

3.1. MWReg30-mediated thrombocytopenia

Treatment of wild-type and γ R knockout strains with MWReg30 (0.05–0.4 mg/kg) resulted in dose-dependent thrombocytopenia in all strains. The maximal reduction of platelet counts was reached within 3–12 h post dosing. Platelet counts returned to baseline levels within 3 days post dosing (Figure 2). The % reduction in platelet counts at nadir, relative to baseline, differed between the strains and across the dose levels. The reduction in platelet counts at 0.4 mg/kg was ~93%, 75%, and 61% for γ R11b(-/-) mice, control mice, and γ R111(-/-) mice. The extent of induced thrombocytopenia was much less severe for the γ R111(-/-) mice relative to the other strains, at all doses (Figure 2). Nadir % platelet counts were 28.6 ± 5.0 , 88.7 ± 16.6 , and 25.3 ± 6.1 % ($p < 0.0001$) at 0.05 mg/kg, 28.4 ± 13.7 , 56.7 ± 5.1 , and 20.6 ± 9.5 % ($p < 0.0001$) at 0.2 mg/kg, and 24.9 ± 7.2 , 38.7 ± 7.5 , and 7.4 ± 2.2 % ($p < 0.0001$) at 0.4 mg/kg. A significant difference in the magnitude of thrombocytopenia between C57BL/6 and γ R11b(-/-) mice was observed at the 0.4 mg/kg dose, but not at 0.5 or 0.1 mg/kg doses.

At the end of forward covariate selection, strain was a significant predictor of both ED_{50} and E_{max} (p -value < 0.00001). However, at the end of backward elimination ($\alpha = 0.001$), only ED_{50} was shown to exhibit a significant relationship with strain ($p = 0.0043$). The final multivariable model-fitted E_{max} and ED_{50} values are summarized in Table 1. E_{max} and ED_{50} parameters were estimated with good precision. The γ R11b(-/-) strain was most sensitive to MWReg30 treatment ($ED_{50} = 0.00232$ mg/kg), followed by the wild type strain ($ED_{50} = 0.00854$ mg/kg), and then the γ R111(-/-) strain ($ED_{50} = 0.156$ mg/kg).

3.2. Effect of iodination on MWReg30-mediated thrombocytopenia

Iodination of MWReg30 did not affect MWReg30-induced thrombocytopenia in mice. As shown in Figure 3, treating groups of Swiss Webster mice with 0.2 mg/kg ^{127}I -MWReg30 or 0.2 mg/kg MWReg30 resulted in very similar effects on platelet counts. Nadir % initial platelet counts were 49.2 ± 14.9 % vs. 54.7 ± 1.4 % ($p = 0.56$) and raw platelet counts were 554 ± 221 k/ μL vs. 591 ± 29 k/ μL , $p = 0.79$, for ^{127}I -MWReg30 vs. MWReg30. Platelet counts returned to baseline within 3 days post dosing. The areas of thrombocytopenia were 94.6 ± 12.5 vs. 99.5 ± 9.99 (% \times day) ($p = 0.62$) for the ^{127}I -MWReg30 and MWReg30 treated groups. This validation that iodination does not influence MWReg30-mediated thrombocytopenia enabled confident use of ^{125}I -MWReg30 for characterizing of MWReg30 pharmacokinetics and tissue distribution, minimizing concerns of the effect of iodination on MWReg30 binding or function.

3.3. MWReg30 pharmacokinetics and tissue disposition

MWReg30 plasma concentration vs. time profiles are illustrated in Figure 4. Biexponential disposition of MWReg30 was observed in all strains, at each dose level. MWReg30 plasma concentration increased in direct proportion with dose, indicating linear pharmacokinetics (Figure 4). No significant differences in dose-normalized AUC and NCA-estimated pharmacokinetics parameters were observed (Table 2). Plasma $AUC_{0-10\text{days}} \pm \text{SD}$ (nM \times d) for MWReg30 were: 5.24 ± 0.68 , 5.51 ± 0.24 , and 5.39 ± 1.05 at 0.04 mg/kg and 12.7 ± 0.5 , 13.6 ± 1.1 , and 14.5 ± 2.0 at 0.1 mg/kg in C57BL/6, γ R111(-/-), and γ R11b(-/-) mice. MWReg30 plasma clearance values (mL/day/kg) were 31.4 ± 6.0 , 29.7 ± 1.5 , 30.5 ± 6.4 at 0.04 mg/kg and 37.5 ± 3.4 , 36.0 ± 12.0 , 28.9 ± 5.4 at 0.1 mg/kg in C57BL/6, γ R111(-/-), and γ R11b(-/-) mice. All mice from the γ R11b(-/-) 0.4 mg/kg group died within 24h post

injection, consistent with hyper-sensitivity to MWReg30 in this strain. Therefore, no pharmacokinetic parameters were reported for this strain at the 0.4 mg/kg dose.

Comparison of tissue to blood concentration ratios did not show any significant differences in the tissue distribution of MWReg30 between C57BL/6, Fc γ RI/RIII(-/-), and Fc γ RIIb(-/-) mice (Figure 5). Higher concentrations of MWReg30 were observed in highly perfused organs and organs associated with “leaky” vasculature (i.e., spleen, lung); lower concentrations were found for organs with low rates of perfusion (muscle, fat, and thymus). In organs associated with cell-types expressing Fc γ R, no significant differences in MWReg30 concentrations were observed. For example, tissue:blood concentration ratios were 0.541 ± 0.086 , 0.56 ± 0.0839 , and 0.4391 ± 0.0371 ($p=0.169$) for the spleen, 0.203 ± 0.049 , 0.531 ± 0.281 , and 0.146 ± 0.0186 ($p=0.054$) for the liver, 0.369 ± 0.0182 , 0.381 ± 0.0145 , and 0.438 ± 0.068 ($p=0.411$) for the lung, 0.155 ± 0.05 , 0.143 ± 0.006 , and 0.144 ± 0.007 ($p=0.868$) for the bone and 0.129 ± 0.014 , 0.166 ± 0.03 , and 0.138 ± 0.053 ($p=0.411$) for the thymus, in C57BL/6, Fc γ RI/RIII(-/-), and Fc γ RIIb(-/-) mice. More than 95% of the radioactivity associated with collected blood samples on day 14 was precipitated with treatment of plasma with TCA, thus indicating that the plasma samples were free from significant quantities of low-molecular weight radiolabeled catabolites.

MWReg30 plasma data were characterized using the base model structure shown in Figure 1. The final model parameter estimates are reported in Table 3. All model parameters were estimated with moderate to high precision. Based on the covariate forward selection analysis, strain was not a significant predictor of any of the tested pharmacokinetic parameters. Hence, one estimate for each parameter was considered for all strains in the final model. Goodness-of-fit plots for MWReg30 plasma data are shown in Figure 6. As shown in the figure, the model described the data reasonably well. The model predicted and observed data were along the line of unity. Visual predictive check plots are shown in Figure 7. For all dose levels, the observed data were well captured by the simulated prediction interval. The observed data were in line with the population predicted median concentrations at all doses, in all strains.

4. Discussion

The main objective of the current work was to evaluate the role of Fc γ R on the pharmacokinetics and pharmacodynamics of MWReg30, an anti-platelet antibody, through the use of Fc γ R-knockout mice. Fc γ R knockout mice have been previously employed to characterize the role of Fc γ R in the initiation or in the inhibition of immunomodulatory effects of antibodies (Nimmerjahn and Ravetch, 2006, 2008; Siberil et al., 2007; Tarasenko et al., 2007). Knocking out Fc γ R receptors was found to abrogate effector cell functions *in vitro* and immune responses *in vivo* (Gessner et al., 1998; Takai et al., 1994). The Fc γ R-dependent phagocytosis of IgG1 was found to be muted in γ chain and Fc γ RIII knockout strains.

MWReg30 is a rat IgG1 antibody that binds to mice glycoprotein (GP) IIb (CD41). GPIIb is associated with GPIIIa, forming the GPIIb/IIIa complex in mice. The complex is important in platelet adhesion and aggregation. GPIIb is expressed on platelets, megakaryocytes, hematopoietic progenitors, bone marrow cells, and mast cells (Berlanga et al., 2005; Soligo et al., 1989). The interaction of MWReg30 with GPIIb on platelets led to a dose proportional increase in platelet destruction, with substantial differences observed between the control mice and the knockout strains. Population modeling demonstrated that the Fc γ RIIb(-/-) mice are more sensitive to MWReg30-induced thrombocytopenia, relative to C57BL/6 or the Fc γ RI/RIII(-/-) mice. Approximately 67- and 3.6-fold higher MWReg30 doses are

required to achieve the 50% inhibition in the Fc γ RI/RIII(-/-) and C57BL6 mice, compared to Fc γ RIIb(-/-) mice.

Assessment of the MWReg30 plasma pharmacokinetics and tissue distribution, across all strains, failed to demonstrate a significant influence of Fc γ R on MWReg30 disposition. MWReg30 demonstrated linear pharmacokinetics, with clear dose-proportionality across the dose-range that was investigated. There were no signs indicating target-mediated mAb elimination, and MWReg30 tissue concentrations were very similar across the mouse strains. Population modeling, with a two compartment model, was employed to characterize the plasma concentration vs. time data. Covariate analysis with forward selection showed that strain was not a significant predictor of inter-animal variability in any of the model parameters. Model parameters were all estimated with high precision (%SEM < 10%).

The profound thrombocytopenia induced by MWReg30, and the lack of target-mediated elimination, indicates that only a small fraction of the MWReg30 dose is eliminated with the destruction of platelets. Other pathways of antibody elimination (e.g., catabolism of unbound MWReg30 in vascular endothelial cells) (Lobo et al., 2004; Wang et al., 2008) are likely to be much more significant relative to the rate of mAb elimination through Fc γ R-mediated phagocytosis of opsonized platelets. Of note, it is possible that following phagocytosis of opsonized platelets, MWReg30 dissociates from GPIIb, and is “recycled” to plasma via the IgG protection receptor, FcRn (Chaparro-Riggers et al., 2012; Igawa et al., 2010; Junghans and Anderson, 1996).

The findings from this work showed that Fc γ R knockout significantly affected the degree of anti-platelet antibody induced thrombocytopenia; however, Fc γ R knockout did not affect the plasma or tissue disposition of MWReg30. The lack of effect of Fc γ R knockout on MWReg30 pharmacokinetics is consistent with our earlier report that demonstrated a lack of influence of Fc γ R knockout on the pharmacokinetics of 8C2, a monoclonal IgG1 antibody with high affinity for a soluble ligand (topotecan) (Abuqayyas and Balthasar, 2012, in press). However, based solely on the results obtained with MWReg30 and 8C2, it is not prudent to conclude that Fc γ R are unimportant as determinants of mAb pharmacokinetics in all cases (i.e., for every monoclonal antibody). Nonetheless, our results do provide strong support for the converse argument. As illustrated with 8C2 and MWReg30, it is clear that Fc γ R are not important contributors to the pharmacokinetics of all IgG mAb.

Acknowledgments

This work was supported by funding from the Center for Protein Therapeutics at the State University of New York University at Buffalo, and by NIH grant HL67437.

Abbreviations

IgG	Immunoglobulin G
FcγR	Fc receptors for IgG
ITP	immune thrombocytopenic purpura
mAbs	monoclonal antibodies
PK	pharmacokinetics
PD	pharmacodynamics
AUC	area under the concentration vs. time profiles
CL	clearance

V_{ss}	volume of distribution at steady-state
NCA	noncompartmental pharmacokinetic analysis
MVOF	mean value of objective function
VPC	visual predictive checks

References

- Abuqayyas L, Balthasar JP. Application of Knockout Mouse Models to Investigate the Influence of FcγR on the Tissue Distribution and Elimination of 8C2, a Murine IgG1 Monoclonal Antibody. *International Journal of Pharmaceutics*. 2012 in press.
- Amigorena S, Bonnerot C. Fc receptor signaling and trafficking: a connection for antigen processing. *Immunol. Rev.* 1999a; 172:279–284. [PubMed: 10631953]
- Amigorena S, Bonnerot C. Fc receptors for IgG and antigen presentation on MHC class I and class II molecules. *Semin. Immunol.* 1999b; 11:385–390. [PubMed: 10625592]
- Berlanga O, Emambokus N, Frampton J. GPIIb (CD41) integrin is expressed on mast cells and influences their adhesion properties. *Exp. Hematol.* 2005; 33:403–412. [PubMed: 15781330]
- Bhatia A, Blades S, Cambridge G, Edwards JC. Differential distribution of Fc gamma RIIIA in normal human tissues and co-localization with DAF and fibrillin-1: implications for immunological microenvironments. *Immunology.* 1998; 94:56–63. [PubMed: 9708187]
- Bordessoule D, Jones M, Gatter KC, Mason DY. Immunohistological patterns of myeloid antigens: tissue distribution of CD13, CD14, CD16, CD31, CD36, CD65, CD66 and CD67. *Br. J. Haematol.* 1993; 83:370–383. [PubMed: 7683483]
- Cassel DL, Keller MA, Surrey S, Schwartz E, Schreiber AD, Rappaport EF, McKenzie SE. Differential expression of Fc gamma RIIA, Fc gamma RIIIB and Fc gamma RIIIC in hematopoietic cells: analysis of transcripts. *Mol. Immunol.* 1993; 30:451–460. [PubMed: 8464427]
- Chaparro-Riggers J, Liang H, Devay RM, Bai L, Sutton JE, Chen W, Geng T, Lindquist K, Casas MG, Boustany LM, Brown CL, Chabot J, Gomes B, Garzone P, Rossi A, Strop P, Shelton D, Pons J, Rajpal A. Increasing Serum Half-life and Extending Cholesterol Lowering in Vivo by Engineering Antibody with pH-sensitive Binding to PCSK9. *J Biol Chem.* 2012; 287:11090–11097. [PubMed: 22294692]
- Cines DB, Blanchette VS. Immune thrombocytopenic purpura. *N. Engl. J. Med.* 2002; 346:995–1008. [PubMed: 11919310]
- Deng R, Balthasar JP. Pharmacokinetic/pharmacodynamic modeling of IVIG effects in a murine model of immune thrombocytopenia. *J. Pharm. Sci.* 2007; 96:1625–1637. [PubMed: 17238194]
- Garg A, Balthasar JP. Physiologically-based pharmacokinetic (PBPK) model to predict IgG tissue kinetics in wild-type and FcRn-knockout mice. *J. Pharmacokinet. Pharmacodyn.* 2007; 34:687–709. [PubMed: 17636457]
- Gessner JE, Heiken H, Tamm A, Schmidt RE. The IgG Fc receptor family. *Ann. Hematol.* 1998; 76:231–248. [PubMed: 9692811]
- Igawa T, Ishii S, Tachibana T, Maeda A, Higuchi Y, Shimaoka S, Moriyama C, Watanabe T, Takubo R, Doi Y, Wakabayashi T, Hayasaka A, Kadono S, Miyazaki T, Haraya K, Sekimori Y, Kojima T, Nabuchi Y, Aso Y, Kawabe Y, Hattori K. Antibody recycling by engineered pH-dependent antigen binding improves the duration of antigen neutralization. *Nat Biotechnol.* 2010; 28:1203–1207. [PubMed: 20953198]
- Ivan E, Colovai AI. Human Fc receptors: critical targets in the treatment of autoimmune diseases and transplant rejections. *Hum. Immunol.* 2006; 67:479–491. [PubMed: 16829303]
- Junghans RP, Anderson CL. The protection receptor for IgG catabolism is the beta2-microglobulin-containing neonatal intestinal transport receptor. *Proc Natl Acad Sci U S A.* 1996; 93:5512–5516. [PubMed: 8643606]
- Lobo ED, Hansen RJ, Balthasar JP. Antibody pharmacokinetics and pharmacodynamics. *Journal of Pharmaceutical Sciences.* 2004; 93:2645–2668. [PubMed: 15389672]

- McDonagh CF, Kim KM, Turcott E, Brown LL, Westendorf L, Feist T, Sussman D, Stone I, Anderson M, Miyamoto J, Lyon R, Alley SC, Gerber HP, Carter PJ. Engineered anti-CD70 antibody-drug conjugate with increased therapeutic index. *Mol. Cancer Ther.* 2008; 7:2913–2923. [PubMed: 18790772]
- Mould DR, Green B. Pharmacokinetics and pharmacodynamics of monoclonal antibodies: concepts and lessons for drug development. *BioDrugs.* 2010; 24:23–39. [PubMed: 20055530]
- Nimmerjahn F, Bruhns P, Horiuchi K, Ravetch JV. FcγRIV: a novel FcR with distinct IgG subclass specificity. *Immunity.* 2005; 23:41–51. [PubMed: 16039578]
- Nimmerjahn F, Ravetch JV. Fcγ receptors: old friends and new family members. *Immunity.* 2006; 24:19–28. [PubMed: 16413920]
- Nimmerjahn F, Ravetch JV. Fcγ receptors as regulators of immune responses. *Nat. Rev. Immunol.* 2008; 8:34–47. [PubMed: 18064051]
- Nishio S, Yamamoto T, Kaneko K, Tanaka-Matsumoto N, Muraoka S, Kaburaki M, Kusunoki Y, Takagi K, Kawai S. Pharmacokinetic study and Fcγ receptor gene analysis in two patients with rheumatoid arthritis controlled by low-dose infliximab. *Mod. Rheumatol.* 2009; 19:329–333. [PubMed: 19255827]
- Ravetch JV, Bolland S. IgG Fc receptors. *Annu. Rev. Immunol.* 2001; 19:275–290. [PubMed: 11244038]
- Siberil S, Dutertre CA, Fridman WH, Teillaud JL. FcγR: The key to optimize therapeutic antibodies? *Crit. Rev. Oncol. Hematol.* 2007; 62:26–33. [PubMed: 17240158]
- Soligo D, Cattoretti G, Colombi M, Polli N, Capsoni F, Rilke F, Delilieri GL. Bone marrow and tissue expression of gpIIb/IIIa, LFA-1, Mac-1 and gp150,95 glycoproteins. *Eur. J. Haematol.* 1989; 42:173–181. [PubMed: 2645166]
- Tabrizi M, Bornstein GG, Suria H. Biodistribution mechanisms of therapeutic monoclonal antibodies in health and disease. *AAPS J.* 2010; 12:33–43. [PubMed: 19924542]
- Tabrizi MA, Tseng CM, Roskos LK. Elimination mechanisms of therapeutic monoclonal antibodies. *Drug Discov. Today.* 2006; 11:81–88. [PubMed: 16478695]
- Takai T, Li M, Sylvestre D, Clynes R, Ravetch JV. Fcγ chain deletion results in pleiotropic effector cell defects. *Cell.* 1994; 76:519–529. [PubMed: 8313472]
- Tarasenko T, Dean JA, Bolland S. FcγRIIB as a modulator of autoimmune disease susceptibility. *Autoimmunity.* 2007; 40:409–417. [PubMed: 17729034]
- Tuijnman WB, Van Wichen DF, Schuurman HJ. Tissue distribution of human IgG Fc receptors CD16, CD32 and CD64: an immunohistochemical study. *APMIS.* 1993; 101:319–329. [PubMed: 8323742]
- Van de Winkel JG, Capel PJ. Human IgG Fc receptor heterogeneity: molecular aspects and clinical implications. *Immunol. Today.* 1993; 14:215–221. [PubMed: 8517920]
- Van Leeuwen EF, Van der Ven JT, Engelfriet CP, Von Dem Borne AE. Specificity of autoantibodies in autoimmune thrombocytopenia. *Blood.* 1982; 59:23–26. [PubMed: 7032627]
- Wang W, Wang EQ, Balthasar JP. Monoclonal antibody pharmacokinetics and pharmacodynamics. *Clin Pharmacol Ther.* 2008; 84:548–558. [PubMed: 18784655]
- Zuckier LS, Georgescu L, Chang CJ, Scharff MD, Morrison SL. The use of severe combined immunodeficiency mice to study the metabolism of human immunoglobulin G. *Cancer.* 1994; 73:794–799. [PubMed: 8306262]

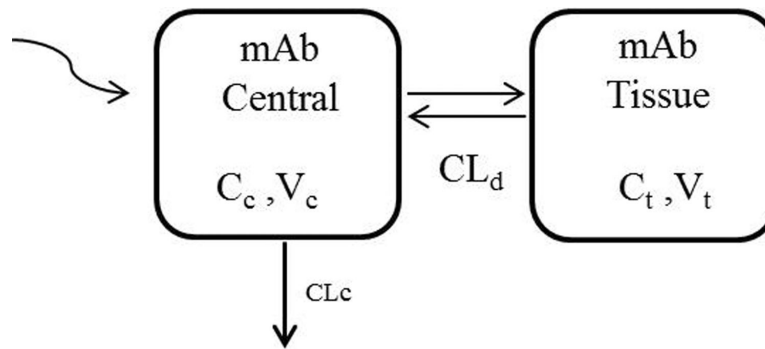


Fig. 1. Schematic representation of the pharmacokinetic model structure for MWReg30 disposition

CL_c represents linear clearance from the central compartment, and CL_d is the distribution clearance between the central and peripheral compartments. V_c and V_t are the volumes of distribution of the central and peripheral compartments.

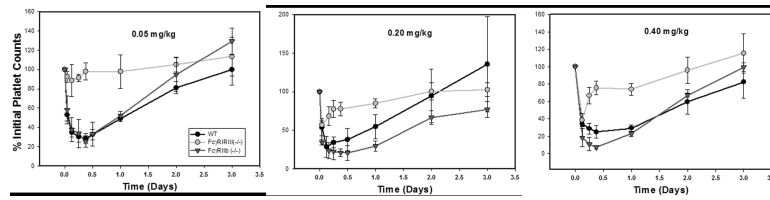


Fig. 2. MWReg30-mediated thrombocytopenia in C57BL/6, FcγRI/RIII(-/-), and FcγRIIb(-/-) mice

Platelet count data are presented following MWReg30 doses of 0.05 mg/kg, 0.2 mg/kg, and 0.4 mg/kg, administered to C57BL/6 wild-type mice (WT), FcγRI/RIII(-/-) mice, and FcγRIIb(-/-) mice. Platelet counts were determined at several time points up to 3 days, and normalized by the baseline platelet counts. Symbols represent the mean % platelet counts, relative to pretreatment values, and error bars represent the standard deviation about the mean (n=5–7 mice per strain per dose). Relative to wild-type mice, FcγRI/RIII(-/-) mice demonstrated reduced sensitivity to MWReg30 and FcγRIIb(-/-) mice demonstrated increased sensitivity to MWReg30.

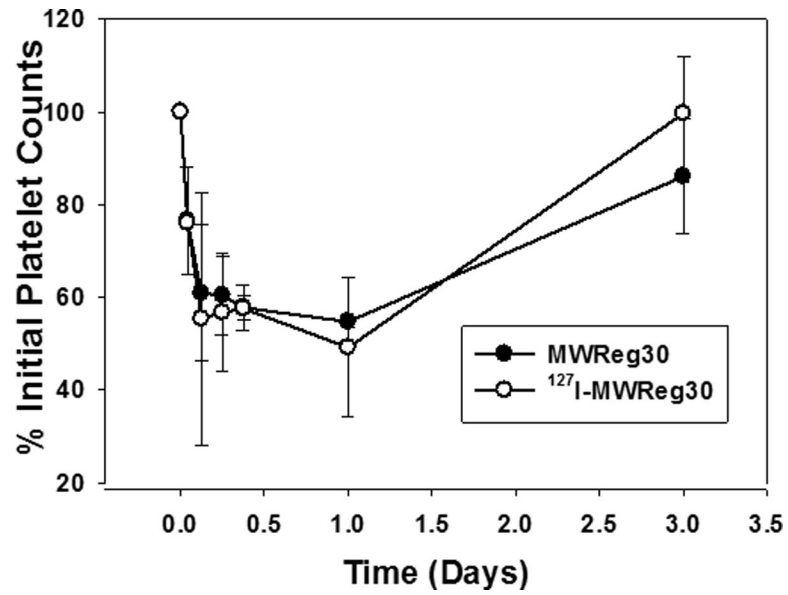


Fig. 3. Effects of iodination on MWReg30-mediated thrombocytopenia
Swiss Webster mice were treated with 0.2 mg/kg MWReg30 or ¹²⁷I-MWReg30. Platelet counts were normalized by the baseline platelet counts. Symbols represent the mean % platelet counts, relative to pretreatment values, and error bars represent the standard deviation about the mean (n=3 mice per group). The two profiles are essentially superimposed. Iodination did not affect MWReg30 induced thrombocytopenia.

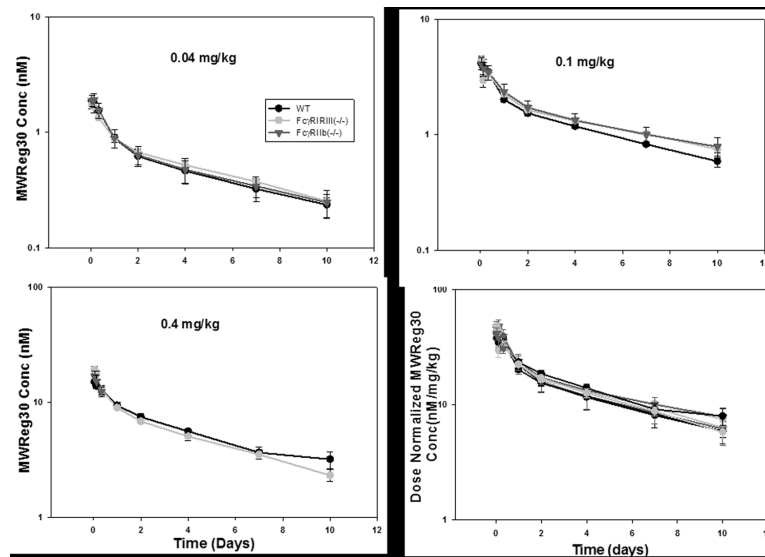


Fig. 4. MWReg30 plasma pharmacokinetics

^{125}I -MWReg30 was injected intravenously at 0.04, 0.1, and 0.4 mg/kg into C57BL/6 wild type (WT), Fc γ RI/RIII(-/-), and Fc γ RIIb(-/-) mice. MWReg30 mean plasma concentrations (nM) following doses of 0.04, 0.1, and 0.4 mg/kg are represented by symbols. Error bars indicate the standard deviation associated with each mean concentration (n=3–5/dose/strain). The plot depicts the dose-normalized MWReg30 concentration (nM/mg/kg) vs. time profiles at 0.04, 0.1, and 0.4 mg/kg in all mouse strains at all doses. The symbols represent mean dose normalized MWReg30 concentrations. Error bars represent the standard deviation associated with mean concentration/dose. Relative to results found in control mice, MWReg30 pharmacokinetics were not altered in Fc γ RI/RIII(-/-) mice or in Fc γ RIIb(-/-) mice.

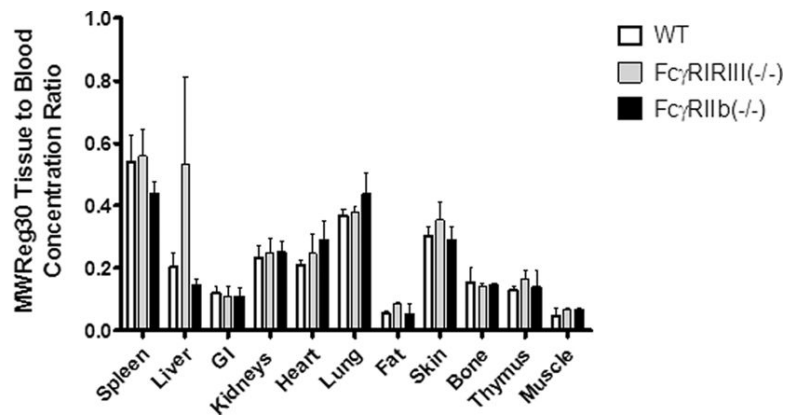


Fig. 5. MWReg30 tissue distribution

MWReg30 tissue to blood concentration ratios were determined following necropsy, 14 days after administration of 0.1 mg/kg MWReg30 to C57BL/6 mice (WT), Fc γ RI/RIII(-/-) mice, and Fc γ RIIb(-/-) mice. Bars represent mean concentration ratios and the error bars indicate the standard deviation of the ratios. Ratios were compared statistically using one way ANOVA with Bonferroni's multiple comparison. Relative to results found in control mice, MWReg30 tissue concentrations were not altered in Fc γ RI/RIII(-/-) mice or in Fc γ RIIb(-/-) mice.

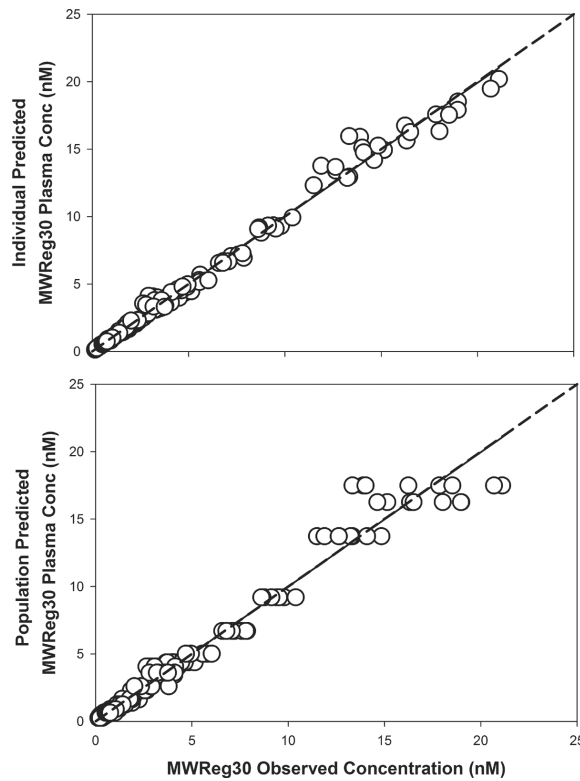


Fig. 6. Goodness-of-fit plots for MWReg30 plasma concentrations

Scatter plots and regression lines (solid) for MWReg30 observed and predicted concentrations in plasma. Shown are MWReg30 plasma individual predictions vs. observed values ($r^2=0.99$), and MWReg30 plasma population predictions vs. observed values ($r^2=0.97$). The dotted lines represent the line of identity.

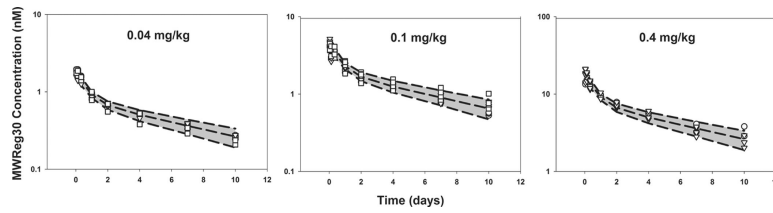


Fig. 7. Visual predictive check

Visual predictive check were performed using data simulated with the final pharmacokinetic model. The shaded area represents the confidence interval (CI) for the 5th, 50th, and 95th percentiles of the simulated data. Observed data are shown for (°) wild type mice, (!) FcγRI/RIII(-/-) mice, and (□) FcγRIIb(-/-) mice, following doses of 0.04, 0.1, 0.4 mg/kg.

Table 1

Parameter estimates for analysis of relationships between MWReg30 dose and nadir platelet counts

Parameter (unit)	Definition	Estimate	%SEM
E_{\max} (%)	Maximal achieved effect	81.0	3.3
ED_{50} (mg/kg) (wild type)	The dose associated with 50% change in effect	0.00854	39.4
Additive shift in ED_{50} for Fc γ R1R111(-/-)		+0.147	17.2
Additive shift in ED_{50} for Fc γ R11b(-/-)		-0.00622	51.0
Inter-animal Variability			
$\sigma^2_{E_{\max}}$	Variance of inter-animal variability for E_{\max}	0.008 (8.9 % CV)	32.6
σ^2_{ED50}	Variance of inter-animal variability for ED_{50}	0.212 (46.0 % CV)	39.9
Residual variability			
σ	Variance of residual error	0.0062 (7.7 % CV)	31.1

Minimum value of the objective function= 258.229

Table 2

Non-compartmental analysis of MWReg30 plasma concentration-time data in C57BL/6, FcγRI/RIII(-/-), and FcγRIIb(-/-) mice

Parameter ^a	Group	0.04 (mg/kg)	0.1 (mg/kg)	0.4(mg/kg)
CL (mL/day/kg)	C57BL/6	31.4 ± 6.0	37.5 ± 3.4	26.0 ± 4.0
	FcγRI/RIII (-/-)	29.7 ± 1.5	36.0 ± 12.0	31.5 ± 2.0
	FcγRIIb (-/-)	30.5 ± 6.4	28.9 ± 5.4	NA ^b
	P-value	0.884	0.308	0.104
AUC _{0-10days} (nM×day)	C57BL/6	5.24 ± 0.68	12.7 ± 0.5	57.5 ± 3.0
	FcγRI/RIII (-/-)	5.51 ± 0.24	13.6 ± 1.1	53.9 ± 1.3
	FcγRIIb (-/-)	5.39 ± 1.05	14.5 ± 2.0	NA
	P-value	0.86	0.235	0.132
V _{ss} (mL/kg)	C57BL/6	243 ± 25	291 ± 11	275 ± 23
	FcγRI/RIII (-/-)	229 ± 28	266 ± 71	197 ± 50
	FcγRIIb (-/-)	244 ± 43	301 ± 42	NA
	P-value	0.755	0.594	0.054

^aParameter values are listed as mean ± standard deviation (n=3-5). % Extrapolated AUC values were less than 25% for all strains at all dose level. P-value of <0.05 was considered significant.

^bMice died within 24 h post MWReg30 injection.

Table 3

Parameter estimates for the final pharmacokinetic model

Parameter (unit)	Definition	Estimate	%SEM
V_c (L/kg)	Central volume of distribution	0.147	2.8
V_t (L/kg)	Volume of tissue compartment	0.143	2.0
CL_d (L/day/kg)	Distribution clearance	0.101	3.9
CL_c (L/day/kg)	Apparent clearance	0.0343	5.6
Inter-animal Variability			
$\sigma^2 V_c$	Variance of inter-animal variability for V_c	0.0218 (14.8 %CV)	39.9
$\sigma^2 CL_d$	Variance of inter-animal variability for CL_d	0.0114 (10.7 %CV)	28.2
$\sigma^2 CL_c$	Variance of inter-animal variability for CL_c	0.208 (38.0 %CV)	76.0
Proportional residual variability			
σ_{prop}	Variance of proportional residual error	0.0068	14.6

Minimum value of the objective function=-586.012